



UNIVERSITY OF LEEDS

This is a repository copy of *Spin relaxation through Kondo scattering in Cu/Py lateral spin valves*.

White Rose Research Online URL for this paper:

<https://eprints.whiterose.ac.uk/93280/>

Version: Supplemental Material

Article:

Batley, JT orcid.org/0000-0001-8752-1439, Rosamond, MC, Ali, M et al. (3 more authors) (2015) Spin relaxation through Kondo scattering in Cu/Py lateral spin valves. *Physical Review B*, 92 (22). 220420(R). ISSN 1098-0121

<https://doi.org/10.1103/PhysRevB.92.220420>

Reuse

Items deposited in White Rose Research Online are protected by copyright, with all rights reserved unless indicated otherwise. They may be downloaded and/or printed for private study, or other acts as permitted by national copyright laws. The publisher or other rights holders may allow further reproduction and re-use of the full text version. This is indicated by the licence information on the White Rose Research Online record for the item.

Takedown

If you consider content in White Rose Research Online to be in breach of UK law, please notify us by emailing eprints@whiterose.ac.uk including the URL of the record and the reason for the withdrawal request.



eprints@whiterose.ac.uk
<https://eprints.whiterose.ac.uk/>

**Spin relaxation through Kondo scattering in Cu/Py lateral spin
valves.**

Supplementary material

J. T. Batley,¹ M. C. Rosamond,² G. Burnell,¹ and B. J. Hickey¹

¹*Physics and Astronomy, University of Leeds, Leeds, UK.*

²*Electronic and Electrical Engineering, University of Leeds, Leeds, UK.*

(Dated: September 2, 2015)

I. FABRICATION

In order to investigate the effect of the spacer channel material quality, specifically the impurity concentration, on the nonlocal signal two sets of LSVs have been fabricated. The two sample sets contain Cu evaporated from different quality source material of 99.99% (four-9s) and 99.9999% (six-9s). The resistivity of the two types of Cu, obtained directly from the LSVs, is shown within the main body of text. This clearly shows the lower purity Cu has a much higher resistivity due to an increased amount of disorder and exhibits a Kondo effect caused by magnetic impurities not present within the six-9s samples.

The four-9s sample set was fabricated initially, with a base pressure of the order 10^{-10} mbar. A scanning electron micrograph of a typical LSV is shown in Fig. 1(a). Both materials are deposited in an UHV evaporation system at different angles to the substrate. The FM is deposited first, with 25 nm of Py evaporated at 45° , followed by the NM, 100 nm of Cu normal to the substrate. Figure 1(b) is a scanning electron micrograph of a typical device. The FM electrodes have widths of 140 nm and 100 nm, with a large nucleation pad on the wider wire to facilitate independent magnetisation reversal. The connecting copper wire has a width of 130 nm and devices were prepared with a range of separations between the magnetic electrodes from 450 nm to 1370 nm.

In order to prepare the six-9s samples the deposition system was vented and the Cu source replaced with the higher purity material. The system was then pumped and baked until an equivalent base pressure to the four-9s samples was achieved. Figure 1(b) shows a typical LSV from the six-9s sample set. Here 20 nm of Py is evaporated at 45° and the widths of the FM electrodes are 115 nm and 90 nm, where the wider wire has the nucleation pad. The Cu spacer has a width and thickness of 100 nm and 85 nm respectively. Although the dimensions of the Cu track are different between the two sample sets this does not contribute significantly to the differences in λ_{Cu} . If surface spin flip scattering[1, 2] were to be a major contribution it would be more dominant within the six-9s sample set as they have both a longer electronic mean free path and smaller cross sectional area compared to the four-9s samples. However, a much larger λ_{Cu} is observed within the six-9s samples indicating that the purity of the Cu, specifically the concentration of magnetic impurities, is a more important factor in the suppression of λ_{Cu} .

Figure 2 shows the resistivity of the Py used during the calculation for the λ_{Cu} and α

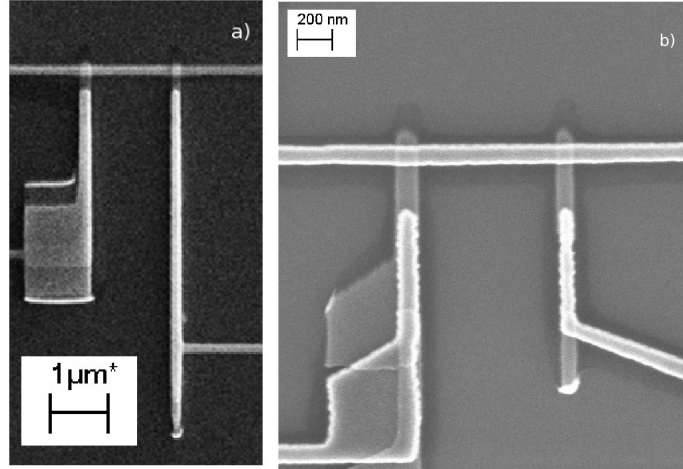


FIG. 1. Scanning electron micrograph showing typical LSVs from the two sample sets. a) four-9s and b) six-9s.

for both sample sets. The resistivities are obtained from samples deposited within similar conditions to the LSVs. There is a slight increase in resistivity for the Py used within the six-9s LSVs due to a reduction in the thickness used and slightly reduced deposition rate. However this will not affect the properties of the Cu on which this study focuses.

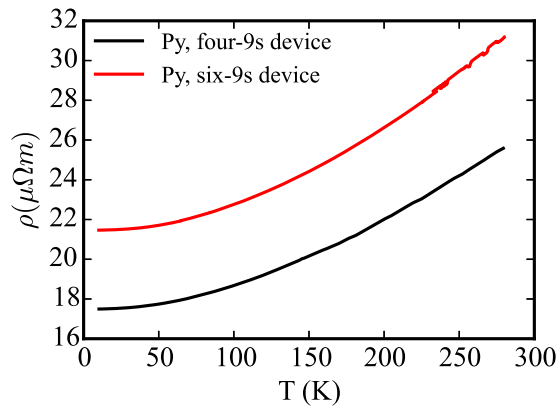


FIG. 2. Resistivities of Py electrodes as a function of temperature used in calculation of λ_{Cu} and α for both sample sets.

II. NONLOCAL MEASUREMENTS

The nonlocal current-voltage characteristics (NLIV) are a powerful tool in observing different transport mechanisms within LSVs. In most studies conventional ac lock-in techniques are used[3–5], however these obscure any dependence the nonlocal signal may have on the direction of the current flow[6]. Throughout this work a dc spin injection method has been used. Figure 3(a) shows a typical NLIV in both the P and AP states. The measured spin signal would be expected to be linear in current and reverse its sign with the current[7, 8]. This is not the case here as the voltage remains positive, independent of the current direction, while also being non-linear. Based on a-priori assumptions we expect the spin-signal to be linear in current whilst thermal and other parasitic effects depend on the power dissipated within the device. From inspection a 2nd order polynomial was chosen to fit to the IV of the form

$$V_{NL} = V_{\beta} + V_s + const. = \beta I^2 + R_s I + const. \quad (1)$$

The constant term accounts for voltage offsets within the experimental apparatus. Here we have made the assumption that the gradient in the linear component of the nonlocal voltage is the spin resistance. This is a formalism that has been adopted throughout the literature where the nonlocal voltage normalised by the injection current produces an effective resistance. Figures 3(b) and (c) show the results of extracting each component from the raw NLIV data. The V_{β} term is obtained from the subtraction of the linear coefficient from the NLIV, producing a voltage signal that varies quadratically with the injection current. It is immediately apparent that there is no correlation with the magnetic state of the LSV, as both P and AP configurations produce the same curve. The absence of a dependence on the alignment of the magnetisation of the FM electrodes indicates V_{β} is not a spin dependent signal. In conjunction with the I^2 behaviour it can be concluded that this is a thermal effect due to joule heating at the injector. We are able to detect this due to the large thermal conductivity of Cu and difference in Seebeck coefficients of Cu and Py. A heat current flows down the Cu wire due to the joule heating within the injector circuit. This raises the temperature of the detector interface with respect to the substrate. Since Cu and Py have very different Seebeck coefficients the detector acts as a thermocouple producing a voltage proportional to the amount of joule heating. This effect is only visible when using

dc injection[6] or observing the higher order harmonics in ac lock-in techniques[9]. The heating at the injector has been shown to affect the magnitude of the spin injection due to the spin-dependent Seebeck effect[10–12] however the current densities in this study are well below those required for this.

The consequence of subtracting the quadratic coefficient from the NLIV data is represented in Fig. 3(c). The end results is a linearly changing voltage with the current that exhibits a strong dependence on the magnetic configuration. This confirms what would be expected of the spin signal from theory[7, 8] and as seen from previous experiments on dc injection[6] where the spin current has a bipolar dependence on the injection current.

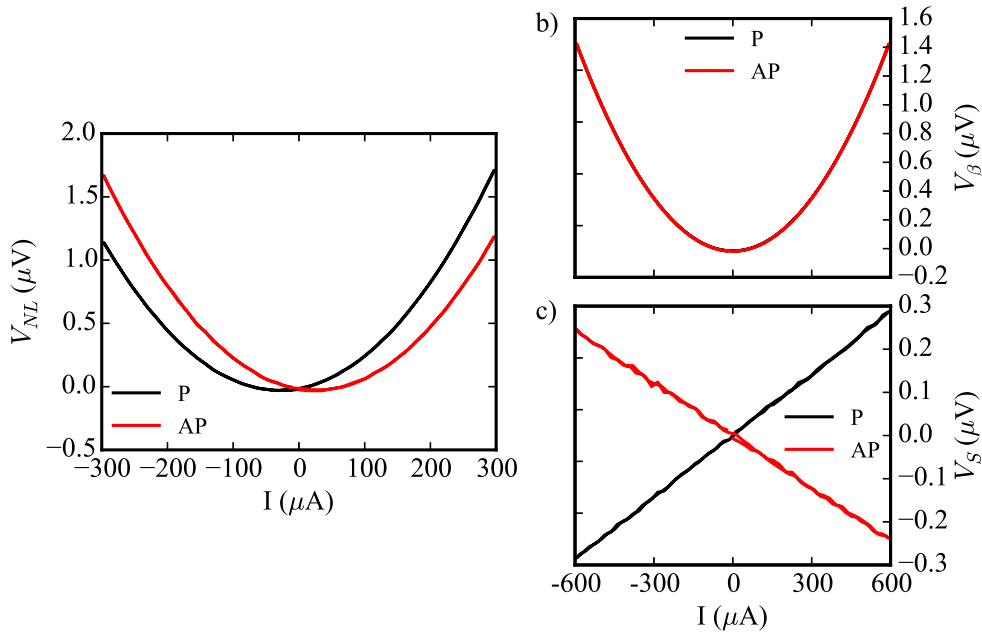


FIG. 3. a) Nonlocal voltage as a function of injection current for P and AP configurations for a four-9s sample with $L = 425$ nm at 30 K. b) Nonlocal voltage after subtraction of linear spin signal showing field independent quadratic background. c) Spin voltage from NLIV after subtraction of quadratic signal.

III. SPIN POLARISATION

When fitting the nonlocal spin signal to obtain λ_{Cu} the effective interface spin polarisation α is a second independent fitting parameter. Figure 4 shows the obtained values for α as a

function of temperature for both four-9s and six-9s samples. The two sample sets show very similar magnitudes and temperature dependence. As the temperature is reduced from 300 K α increases due to a reduction of magnon population, which cause spin mixing within the Py. However both show a peak around 70 K and a reduction of the interface polarisation at low temperatures. This has been observed else where and correlated to diffusion of the FM into the NM at the interface with the formation of randomly orientated local moments dephasing the spin accumulation and reducing the effective interface polarisation through the Kondo effect[5].

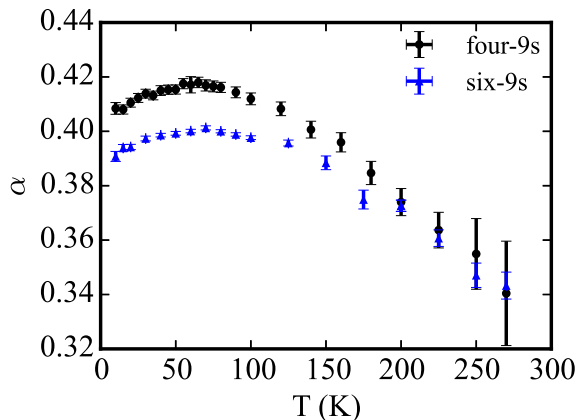


FIG. 4. Effective interface polarisation (α) calculated from fits to the 1-D spin diffusion model for the two sample sets.

IV. ORIGIN OF THE RESISTIVITY MINIMUM

In many systems the observation of a resistivity minimum indicates the presence of weak localization. Localization effects, including Anderson localisation, are present in samples with a significant amount of disorder that is usually identified by the resistivity and its temperature dependence. However, the resistivity of our Cu is $2 \mu\Omega cm$ (i.e. $\ll 50 \mu\Omega cm$ the Mooij critical value), and the temperature dependence of ρ is that of bulk Cu and therefore does not display features associated with weak localization. The observation of Anderson localization can occur in systems with reduced dimensionality provided the resistivity is sufficiently high[13, 14]. A wire with resistivity $100 \mu\Omega cm$ and radius of 25 nm will approach the one-dimensional regime and display localization effects below 1 K. Since the Cu wires

used in our study have a much larger cross sectional area of 1.410^{-14} m² and resistivity 50 times smaller, the critical temperature for localization effects is far below our experimental range.

Weak anti-localization effects due to spin orbit coupling, meanwhile, can be observed in clean materials[15] but these show the opposite sign of $d\rho/dT$ compared to our experiment, and so can be discounted.

This analysis leaves the Kondo effect as the only viable candidate to describe the change in the resistivity. Cu-Fe is a very well characterised Kondo system that typically displays a resistance minimum in this temperature region. The concentration of Fe impurities has been measured by the manufacturers of the source material (12 ppm) and agrees with our determination using the Kondo theory (4 ppm). The smaller concentration in the evaporated material is unsurprising and caused by differential evaporation of the two elements. In addition, our conclusion does not depend on the absolute value for the impurity concentrations. Furthermore, the only other impurity of significant levels is Ni (15 ppm). However, since the Kondo temperature of Ni in Cu is >1000 K the moments are fully screened and do not contribute to the Kondo effect[16].

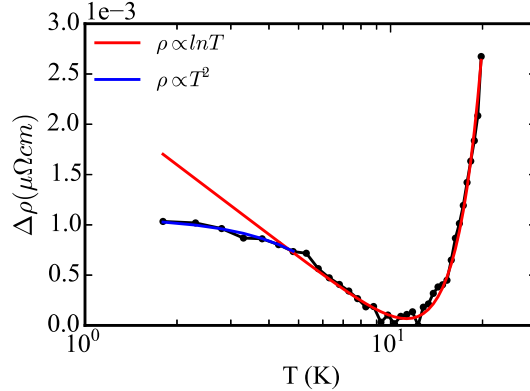


FIG. 5. $\Delta\rho = \rho(T) - \rho(T_{min})$ at low temperature for the four-9s samples. Two fits show the cross over between the $\ln T$ and T^2 regimes as electron-electron interactions begin to dominate at very low temperatures.

A smoking gun for the Kondo effect is the observation of electron-electron interactions. The temperature dependence of the Kondo effect has been shown to exhibit a logarithmic term due to magnetic impurity scattering that becomes a T^2 dependence well below the Kondo temperature where screening of the impurities and electron-electron interactions be-

come dominant[17]. We see exactly this with a crossover between the two regimes around 4 K as shown in Figure 5. It is at this temperature that the original description by Kondo[18] using second order perturbation theory breaks down. However, the $\ln T$ temperature dependence is used in the analysis of the spin flip scattering as these measurements are at temperatures far from when screening effects occur and the result from perturbation theory is valid.

-
- [1] T. Kimura, T. Sato, and Y. Otani, Phys. Rev. Lett., **100**, 066602 (2008).
 - [2] G. Mihajlović, J. E. Pearson, S. D. Bader, and A. Hoffmann, Phys. Rev. Lett., **104**, 237202 (2010).
 - [3] F. Jedema, M. Nijboer, A. Filip, and B. van Wees, Phys. Rev. B, **67**, 085319 (2003).
 - [4] T. Kimura and Y. Otani, Phys. Rev. Lett., **99**, 196604 (2007).
 - [5] L. O'Brien, M. J. Erickson, D. Spivak, H. Ambaye, R. J. Goyette, V. Lauter, P. A. Crowell, and C. Leighton, Nat. Comms., **5** (2014).
 - [6] F. Casanova, A. Sharoni, M. Erekhinsky, and I. Schuller, Phys. Rev. B, **79**, 184415 (2009).
 - [7] T. Valet and A. Fert, Phys. Rev. B, **48**, 7099 (1993).
 - [8] S. Takahashi and S. Maekawa, Sci. Technol. Adv. Mater., **9**, 014105 (2008).
 - [9] F. L. Bakker, A. Slachter, J.-P. Adam, and B. J. van Wees, Phys. Rev. Lett., **105**, 136601 (2010).
 - [10] A. Slachter, F. L. Bakker, J.-P. Adam, and B. J. van Wees, Nat. Phys., **6**, 879 (2010).
 - [11] M. Erekhinsky, F. Casanova, I. K. Schuller, and A. Sharoni, Appl. Phys. Lett., **100**, 212401 (2012).
 - [12] S. Hu and T. Kimura, Phys. Rev. B, **87**, 014424 (2013).
 - [13] P. A. Lee and T. V. Ramakrishnan, Reviews of Modern Physics, **57**, 287 (1985).
 - [14] N. Giordano, W. Gilson, and D. E. Prober, Phys. Rev. Lett., **43**, 725 (1979).
 - [15] Y. Niimi, D. Wei, H. Idzuchi, T. Wakamura, T. Kato, and Y. Otani, Phys. Rev. Lett., **110**, 016805 (2013).
 - [16] J. A. Mydosh, *Spin Glasses: An experimental introduction* (Taylor and Francis, 1993).
 - [17] T. A. Costi, A. C. Hewson, and V. Zlatic, J. Phys.: Condens. Matter, **6**, 2519 (1994).
 - [18] J. Kondo, Progr. Theoret. Phys., **32**, 37 (1964).